Eur. Phys. J. C 44, 195–203 (2005)
Digital Object Identifier (DOI) 10.1140/epjc/s2005-02363-1

THE EUROPEAN PHYSICAL JOURNAL C

One-loop electroweak factorizable corrections for the Higgsstrahlung at a linear collider*

F. Jegerlehner[1,a], K. Kołodziej[2,b], T. Westwański[2,c]

[1] Deutsches Elektronen-Synchrotron DESY, Platanenallee 6, 15738 Zeuthen, Germany
[2] Institute of Physics, University of Silesia, ul. Uniwersytecka 4, 40007 Katowice, Poland

Received: 17 March 2005 / Revised version: 30 March 2005 /
Published online: 30 August 2005 –

Abstract. We present standard model predictions for the four-fermion reaction $e^+e^- \to \mu^+\mu^-\bar{b}b$ being one of the best detection channels of a low-mass Higgs boson produced through the Higgsstrahlung mechanism at a linear collider. We include leading virtual and real QED corrections due to initial state radiation and a modification of the Higgs–$b\bar{b}$ Yukawa coupling, caused by the running of the b-quark mass, for $e^+e^- \to \mu^+\mu^-\bar{b}b$. The complete $\mathcal{O}(\alpha)$ electroweak corrections to Z–Higgs production and to the Z-boson decay width, as well as the remaining QCD and EW corrections to the Higgs decay width, as can be calculated with the program `HDECAY`, are taken into account in the double-pole approximation.

1 Introduction

Although the Higgs boson has not yet been discovered, its mass m_H can be constrained in the framework of the standard model (SM) by the virtual effects it has on precision electroweak (EW) observables. Recent global fits to all precision EW data [1] give a central value of $m_H = 114^{+56}_{-40}$ GeV and an upper limit of 241 GeV, both at 95% confidence level (CL), in agreement with combined results on the direct searches for the Higgs boson at LEP that led to a lower limit of 114.4 GeV at 95% CL [2]. These constraints indicate the mass range where the SM Higgs boson should be sought. If the Higgs boson exists, it is most probably that it will be discovered at the Large Hadron Collider (LHC), but its properties can be best investigated in a clean experimental environment of e^+e^- collisions at a future International Linear Collider (ILC) [3].

The main mechanisms for SM Higgs boson production at the ILC are the Higgsstrahlung reaction

$$e^+e^- \to ZH\,, \tag{1}$$

the WW fusion

$$e^+e^- \to \nu_e\bar{\nu}_e W^*W^* \to \nu_e\bar{\nu}_e H\,, \tag{2}$$

* Work supported in part by the Polish State Committee for Scientific Research in years 2004–2006 as a research grant, by the European Community's Human Potential Program under contracts HPRN-CT-2000-00149 Physics at Colliders and CT-2002-00311 EURIDICE, and by DFG under Contract SFB/TR 9-03.

[a] e-mail: fred.jegerlehner@desy.de
[b] e-mail: kolodzie@us.edu.pl
[c] e-mail: twest@server.phys.us.edu.pl

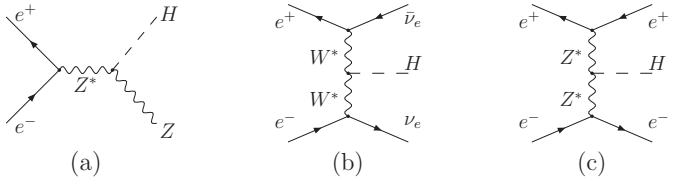

Fig. 1a–c. Feynman diagrams of reactions (1), (2) and (3), respectively

and the ZZ fusion process

$$e^+e^- \to e^+e^-Z^*Z^* \to e^+e^-H\,. \tag{3}$$

The Feynman diagrams of reactions (1), (2), and (3) are depicted in Fig. 1a, 1b, and 1c, respectively.

The cross section of reaction (1) decreases according to the $1/s$ scaling law, while that of reaction (2) grows as $\ln(s/m_H^2)$. Hence, while the Higgsstrahlung dominates Higgs-boson production at low energies, the WW fusion process overtakes it at higher energies. The Higgs-boson production rate through the ZZ fusion mechanism (3) is an order of magnitude smaller than that of process (2). The production of the SM Higgs boson in the intermediate mass range at high-energy e^+e^- colliders through reaction (1) has already been thoroughly studied in the literature [4]. In the present paper, we contribute further to the theoretical analysis of the Higgsstrahlung reaction by taking into account decays of the Z and Higgs bosons, including the EW radiative effects that are most relevant to the production and decay subprocesses. Preliminary results of the present study have already been presented in a conference paper [5].

If the Higgs boson has a mass in the lower part of the range indicated above, say $m_H < 140$ GeV, it would decay

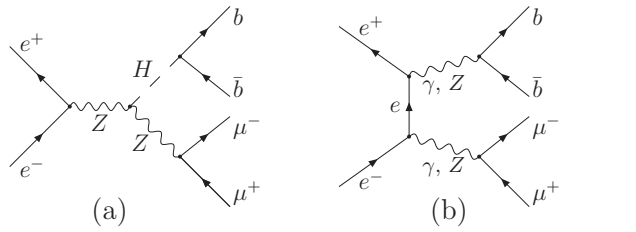

Fig. 2. Examples of the Feynman diagrams of reaction (4): **a** the double resonance signal, **b** and **c** background diagrams

dominantly into a $\bar{b}b$ quark pair. As the Z boson of reaction (1) decays into a fermion–antifermion pair too, one actually observes the Higgsstrahlung through reactions with four fermions in the final state. To be more specific, in the following we will concentrate on a four-fermion channel

$$e^+(p_1) + e^-(p_2) \to \mu^+(p_3) + \mu^-(p_4) + \bar{b}(p_5) + b(p_6)\,, \qquad (4)$$

which is one of the most relevant for detection of (1) at the ILC, and the corresponding bremsstrahlung reaction

$$e^+(p_1) + e^-(p_2) \to \mu^+(p_3) + \mu^-(p_4) + \bar{b}(p_5) + b(p_6) + \gamma(p_7)\,. \qquad (5)$$

In both (4) and (5), the particle four-momenta have been indicated in parentheses. While the final states of reactions (4) and (5) are practically undetectable in hadronic collisions because of the overwhelming QCD background, at the ILC, they should leave a particularly clear signature in a detector. To the lowest order of the SM, in the unitary gauge and neglecting the Higgs-boson coupling to the electron, reactions (4) and (5) receive contributions from 34 and 236 Feynman diagrams, respectively. Typical examples of Feynman diagrams of reaction (4) are depicted in Fig. 2. The Higgsstrahlung signal diagram is shown in Fig. 1a, while the diagrams in Figs. 1b and 1c represent typical background diagrams. The Feynman diagrams of reaction (5) are obtained from those of reaction (4) by attaching an external photon line to each electrically charged particle line. Reactions (4) and (5) are typical examples of the neutral-current four-fermion reactions and the corresponding hard bremsstrahlung reactions which have already been studied for LEP2 and TESLA TDR [3] in the case of massless fermions [6,7] and without neglecting fermion masses [8,9]. Reaction (4) was in particular studied in [10]. It was also considered, among other four-fermion reactions relevant for Higgs-boson production and decay, in a study of the searches for the Higgs boson at LEP2 performed in [11], where references to other works dedicated to the subject can also be found.

To match the precision of data from a high-luminosity linear collider, expected to be better than 1%, it is necessary to include radiative corrections in the SM predictions for reaction (4). Calculation of the complete electroweak (EW) $\mathcal{O}(\alpha)$ corrections to a four-fermion reaction like (4) is a challenging task. Problems encountered in the first attempt at such a complete calculation were described in [12]. Substantial progress in a full one-loop calculation for $e^+e^- \to u\bar{d}\mu^-\bar{\nu}_\mu$ was reported by the GRACE/1-LOOP team [13] and recently results of the first calculation of the complete EW $\mathcal{O}(\alpha)$ corrections to charged-current e^+e^- →four fermion processes have been presented [14]. Another step towards obtaining high-precision predictions for Higgs-boson production, accomplished in [15], was calculations of EW corrections to $e^+e^- \to \nu\bar{\nu}H$, a process related to (4). At the moment, however, there is no complete calculation of the corrections to neutral-current e^+e^- →four fermion processes available that could be included in a Monte Carlo (MC) generator. Therefore it seems natural to include the leading QED corrections and to apply the double-pole approximation (DPA) for the EW $\mathcal{O}(\alpha)$ corrections, as has been done before in [16] in the case of W-pair production at LEP2. This means that we will include the so-called factorizable EW corrections to ZH production (1) and to the subprocesses of the Z and Higgs decay, which are available in the literature.

To the lowest order of the SM, the cross sections of reactions (4) and (5) can be computed with a program `ee4fg` [17]. On the basis of `ee4fg`, we have written a dedicated program `eezh4f` that includes the following radiative corrections to (4):

- the virtual and real soft-photon QED corrections to the on-shell ZH production (1), a universal part of which is utilized for all Feynman diagrams of reaction (4) and combined with the initial-state hard-bremsstrahlung correction of (5), which we refer to as the initial-state radiation (ISR) quantum electrodynamics (QED) correction;
- the weak corrections to Z–Higgs production [18, 19], that is, the infrared (IR) finite part of the complete $\mathcal{O}(\alpha)$ EW correction to (1) and full EW corrections, including hard photon emission, to the Z decay width [20, 21] in the DPA;
- the correction to the Higgs-boson decay width, as can be computed with `HDECAY` [22].

The correction to the partial Higgs-boson decay width $\Gamma_{H\to b\bar{b}}$ is split into two parts: one part is the tree-level partial width $\Gamma^{(0)}_{H\to b\bar{b}}$ parameterized in terms of the running b-quark mass and the other part is the correction term that contains the remaining QCD corrections and the bulk of the EW corrections, as described in [22]. The first part is included in the calculation of reactions (4) and (5) through the corresponding modification of the $H \to b\bar{b}$ Yukawa coupling, while the second part is taken into account in the DPA.

The non-factorizable corrections to (4) have not yet been included in `eezh4f`. However, a comparison with the related process of ZZ production and decay, where the

non-factorizable corrections largely cancel each other in the total cross section [23, 24], may suggest that they are also numerically suppressed for the ZH-mediated four-fermion final states if one integrates over decay angles, and that they should be included in the program if one wants to study differential cross sections, or if one wants to improve the predictions for invariant-mass distributions and similar quantities.

2 Calculation scheme

The corrections listed in the introduction are taken into account in the radiatively corrected total cross section of (4) according to the master formula

$$\int \mathrm{d}\sigma = \int \mathrm{d}\sigma_{\mathrm{Born+r.m.}} + \int_{E_\gamma<E_{\mathrm{cut}}} \mathrm{d}\sigma^{\mathrm{QED\ ISR}}_{\mathrm{virt\ +\ soft,\ univ.}} + \int_{E_\gamma>E_{\mathrm{cut}}} \mathrm{d}\sigma^{\mathrm{QED\ ISR}}_{\mathrm{hard}} + \int \mathrm{d}\sigma^{\mathrm{EW\ DPA}}_{\mathrm{virt,\ finite}} . \quad (6)$$

By $\mathrm{d}\sigma_{\mathrm{Born+r.m.}}$ we denote the effective Born approximation

$$\mathrm{d}\sigma_{\mathrm{Born+r.m.}} = \frac{1}{2s}\left\{\left|M^{4f}_{\mathrm{Born}}\right|^2 + 2\,\mathrm{Re}\left(M^{4f\,*}_{\mathrm{Born}}\,\delta M^{4f}_{\mathrm{r.m.}}\right)\right\}\mathrm{d}\Phi_{4f} , \quad (7)$$

where M^{4f}_{Born} is the matrix element of reaction (4) obtained with the complete set of lowest-order Feynman diagrams, $\delta M^{4f}_{\mathrm{r.m.}}$ is the correction to the amplitude of the signal diagram of Fig. 2a due to the modification $\delta g^{\mathrm{r.m.}}_{Hb\bar{b}}$ of the lowest-order Higgs–$b\bar{b}$ Yukawa coupling $g_{Hb\bar{b}}$ caused by the running of the b-quark mass, $\mathrm{d}\Phi_{4f}$ is the Lorentz-invariant four-particle phase-space element and $4f$ is a shorthand notation for the final state of reaction (4). The correction $\delta M^{4f}_{\mathrm{r.m.}}$ can be written

$$\delta M^{4f}_{\mathrm{r.m.}} = \bar{v}(p_1)\left(A^{(0)}_1\gamma_\mu + A^{(0)}_2\gamma_\mu\gamma_5\right)u(p_2) \times\frac{-g^{\mu\nu}+p^\mu_{34}p^\nu_{34}/M^2_Z}{D_Z(p_{34})D_H(p_{56})}\,\bar{u}(p_4)(a_1\gamma_\nu+a_2\gamma_\nu\gamma_5) \times v(p_3)\,\delta g^{\mathrm{r.m.}}_{Hb\bar{b}}\,\bar{u}(p_6)v(p_5) , \quad (8)$$

where $A^{(0)}_1$ and $A^{(0)}_2$ are the lowest-order invariant amplitudes of the on-shell Higgsstrahlung reaction (1) [18] which read

$$A^{(0)}_i = \frac{g^{(0)}_{HZZ}}{s-M^2_Z}\,a^{(0)}_i, \qquad i=1,2 , \quad (9)$$

and $D_Z(p_{34})$ and $D_H(p_{56})$ are denominators of the Z and Higgs-boson propagators

$$D_Z(p_{34}) = (p_3+p_4)^2 - M^2_Z , \qquad D_H(p_{56}) = (p_5+p_6)^2 - M^2_H , \quad (10)$$

with the complex mass parameters

$$M^2_Z = m^2_Z - im_Z\Gamma_Z, \qquad M^2_H = m^2_H - im_H\Gamma_H . \quad (11)$$

The fixed total widths Γ_Z and Γ_H of the Z and Higgs bosons have been introduced to avoid singularities in the resonant regions of the corresponding propagators. We have also used the complex mass substitution in (9), although the propagator factor of (9) can never become resonant, as we want to keep open the possibility of performing calculations in the complex mass scheme [7], which preserves Ward identities.

To the lowest order of the SM, the vector and axial-vector couplings of the Z boson to leptons, $a^{(0)}_1$, $a^{(0)}_2$, the Higgs-boson coupling to Z, $g^{(0)}_{HZZ}$ of (9) and the Higgs–$b\bar{b}$ Yukawa coupling, $g^{(0)}_{Hbb}$, are given by

$$a^{(0)}_1 = \frac{4s^2_W-1}{4s_Wc_W}\,e_W , \qquad a^{(0)}_2 = \frac{e_W}{4s_Wc_W} , \qquad g^{(0)}_{HZZ} = \frac{e_Wm_Z}{s_Wc_W} , \qquad g^{(0)}_{Hbb} = -\frac{e_Wm_b}{2s_Wm_W} , \quad (12)$$

with the effective electric charge $e_W = (4\pi\alpha_W)^{1/2}$ and electroweak mixing angle θ_W defined by

$$\alpha_W = \sqrt{2}G_\mu m^2_W s^2_W/\pi \quad \text{and} \quad s^2_W = 1 - m^2_W/m^2_Z , \quad (13)$$

where m_W and m_Z are the physical masses of the W and Z boson, respectively. This choice, which is exactly equivalent to the G_μ-scheme of [18], is referred to as a *fixed width scheme* (FWS) in the program. We have introduced the usual shorthand notation $s_W = \sin\theta_W$ and $c_W = \cos\theta_W$ in (12) and (13).

The total widths of (11) are calculated numerically in the framework of the SM: Γ_Z is computed with a program based on [21] and Γ_H is obtained with a program `HDECAY` [22], where both programs include radiative corrections. In order not to violate unitarity it is important that we include exactly the same corrections in the amplitudes of the partial decay widths $\Gamma_{Z\to\mu^+\mu^-}$ and $\Gamma_{H\to b\bar{b}}$.

The program `HDECAY` includes the full massive next-to-leading-order (NLO) QCD corrections close to the thresholds and the massless $\mathcal{O}(\alpha^3_s)$ corrections far above the thresholds. Both regions are related with a simple linear interpolation equation which, for the partial Higgs decay width $\Gamma_{H\to b\bar{b}}$, reads

$$\Gamma_{H\to b\bar{b}} = \left(1-r^2\right)\Gamma_{H\to b\bar{b}}\left(\overline{m}_b(m_H)\right) + r^2\Gamma_{H\to b\bar{b}}(m_b) , \quad \text{with} \quad r = \frac{2m_b}{m_H} , \quad (14)$$

where large logarithms are resummed in the running b-quark mass in the $\overline{\mathrm{MS}}$ renormalization scheme $\overline{m}_b(m_H)$.

By inserting the representations

$$\Gamma_{H\to b\bar{b}}\left(\overline{m}_b(m_H)\right) = \Gamma^{(0)}_{H\to b\bar{b}}\left(\overline{m}_b(m_H)\right) + \Delta\Gamma_{H\to b\bar{b}}\left(\overline{m}_b(m_H)\right), \quad (15)$$

$$\Gamma_{H\to b\bar{b}}(m_b) = \Gamma^{(0)}_{H\to b\bar{b}}(m_b) + \Delta\Gamma_{H\to b\bar{b}}(m_b) , \quad (16)$$

with the lowest-order partial width into the $b\bar{b}$-quark-pair given by

$$\Gamma^{(0)}_{H\to b\bar{b}}(m_b) = 3\frac{{g^{(0)}_{Hb\bar{b}}}^2}{8\pi} m_H \left(1-\frac{4m_b^2}{m_H^2}\right)^{\frac{3}{2}}, \qquad (17)$$

into (14), we obtain the representation

$$\Gamma_{H\to b\bar{b}} = \Gamma^{\text{r.m.}}_{H\to b\bar{b}} + \Delta\Gamma_{H\to b\bar{b}} \qquad (18)$$

for $\Gamma_{H\to b\bar{b}}$. The first term on the right-hand side of (18)

$$\Gamma^{\text{r.m.}}_{H\to b\bar{b}} = \left(1-r^2\right)\Gamma^{(0)}_{H\to b\bar{b}}\Big(\overline{m}_b(m_H)\Big) + r^2\Gamma^{(0)}_{H\to b\bar{b}}(m_b) \qquad (19)$$

contains the correction due to the running of the b-quark mass, while the second term, $\Delta\Gamma_{H\to b\bar{b}}$, incorporates the remaining QCD corrections and EW corrections that are taken into account in HDECAY.

Now, if we write the radiatively corrected Higgs–$b\bar{b}$ Yukawa coupling in the form

$$g_{Hb\bar{b}} = g^{(0)}_{Hb\bar{b}} + \delta g^{\text{r.m.}}_{Hb\bar{b}} + \delta g_{Hb\bar{b}} \qquad (20)$$

and the corrected partial Higgs decay width as

$$\Gamma_{H\to b\bar{b}} = \Gamma^{(0)}_{H\to b\bar{b}}(m_b) \times \left[1+2\,\text{Re}\left(\frac{\delta g^{\text{r.m.}}_{Hb\bar{b}}+\delta g_{Hb\bar{b}}}{g^{(0)}_{Hb\bar{b}}}\right)\right], \qquad (21)$$

then we will obtain the following expressions for the radiative corrections $\delta g^{\text{r.m.}}_{Hb\bar{b}}$ and $\delta g_{Hb\bar{b}}$, assuming that they real,

$$\delta g^{\text{r.m.}}_{Hb\bar{b}} = \frac{\Gamma^{\text{r.m.}}_{H\to b\bar{b}} - \Gamma^{(0)}_{H\to b\bar{b}}(m_b)}{2\Gamma^{(0)}_{H\to b\bar{b}}(m_b)} g^{(0)}_{Hb\bar{b}},$$
$$\delta g_{Hb\bar{b}} = \frac{\Gamma_{H\to b\bar{b}} - \Gamma^{\text{r.m.}}_{H\to b\bar{b}}}{2\Gamma^{(0)}_{H\to b\bar{b}}(m_b)} g^{(0)}_{Hb\bar{b}}. \qquad (22)$$

We see that taking into account the correction $\delta g^{\text{r.m.}}_{Hb\bar{b}}$ in (7) is actually equivalent to replacing m_b in the lowest-order Higgs–$b\bar{b}$ Yukawa coupling of (12) by some effective value of the b-quark mass. The same modification of the Higgs–$b\bar{b}$ Yukawa coupling is done in the soft and hard bremsstrahlung corrections represented by the second and third terms on the right-hand side of (6), respectively.

After having arranged the radiative corrections in the manner just described, the soft bremsstrahlung contribution of (6) can be written as

$$\text{d}\sigma^{\text{QED ISR}}_{\text{virt + soft, univ.}} = \text{d}\sigma_{\text{Born+r.m.}} C^{\text{QED ISR}}_{\text{virt + soft, univ.}}, \qquad (23)$$

where the correction factor $C^{\text{QED ISR}}_{\text{virt + soft, univ.}}$,

$$C^{\text{QED ISR}}_{\text{virt}+\text{soft, univ.}} = \frac{e^2}{2\pi^2} \times \left[\left(\ln\frac{s}{m_e^2}-1\right)\ln\frac{2E_{\text{cut}}}{\sqrt{s}} + \frac{3}{4}\ln\frac{s}{m_e^2}\right], \qquad (24)$$

combines the universal IR singular part of the $\mathcal{O}(\alpha)$ virtual QED correction to the on-shell ZH production process (1) with the soft bremsstrahlung correction to (4), integrated up to the soft-photon energy cut E_{cut}. In (23), e is the electric charge that is given in terms of the fine-structure constant in the Thomson limit α_0, $e=(4\pi\alpha_0)^{1/2}$.

The third term on the right-hand side of (6) represents the initial-state real hard-photon correction to reaction (4), i.e. the lowest-order cross section of reaction (5) with the photon energy cut $E_\gamma > E_{\text{cut}}$, which is calculated taking into account the photon emission from the initial-state particles. It has been checked numerically that the dependence on E_{cut} cancels in the sum of the second and third term on the right-hand side of (6), provided that the real photon coupling to the initial-state fermions is also parameterized in terms of α_0.

Finally, the last integrand on the right-hand side of (6), $\text{d}\sigma^{\text{EW, DPA}}_{\text{virt, finite}}$, is the IR finite part of the virtual EW $\mathcal{O}(\alpha)$ correction to reaction (4) in the DPA. It can be written in the following way

$$\text{d}\sigma^{\text{EW, DPA}}_{\text{virt, finite}} = \frac{1}{2s} \times \left\{\left|M^{(0)}_{DPA}\right|^2 C^{\text{non-univ.}}_{\text{QED}} + 2\,\text{Re}\left(M^{(0)^*}_{DPA}\delta M_{DPA}\right)\right\}\text{d}\Phi_{4f}, \qquad (25)$$

where the lowest-order matrix element $M^{(0)}_{DPA}$ and the one-loop correction δM_{DPA} in the DPA, which are given below, are calculated with the projected four-momenta k_i, $i=3,\ldots,6$, of the final-state particles, except for the denominators of the Z and Higgs-boson propagators. The projected four-momenta are obtained from the four-momenta p_i, $i=3,\ldots,6$, of reaction (4) with a, to some extent arbitrary, projection procedure which will be defined later; $C^{\text{non-univ.}}_{\text{QED}}$ denotes the IR finite non-universal constant part of the $\mathcal{O}(\alpha)$ QED correction that has not been taken into account in (24). It reads

$$C^{\text{QED ISR}}_{\text{non-univ.}} = \frac{e^2}{2\pi^2}\left(\frac{\pi^2}{6}-1\right). \qquad (26)$$

The matrix elements $M^{(0)}_{DPA}$ and δM_{DPA} for the Z and Higgs-boson production and decay of (25) are given by

$$M^{(0)}_{DPA} = -\bar{v}(p_1)\left(A^{(0)}_1\gamma_\mu + A^{(0)}_2\gamma_\mu\gamma_5\right)u(p_2) \times \frac{1}{D_Z(p_{34})D_H(p_{56})}N^\mu_Z N_H, \qquad (27)$$

$$\delta M_{DPA} = -\Big\{\bar{v}(p_1)\Big[\delta A_1\gamma_\mu + \delta A_2\gamma_\mu\gamma_5 + (A_{31}p_{1\mu}+A_{32}p_{2\mu})\not{k}_Z + (A_{41}p_{1\mu}+A_{42}p_{2\mu})\not{k}_Z\gamma_5\Big]u(p_2)\,N^\mu_Z N_H$$

$$+\bar{v}(p_1)\left(A_1^{(0)}\gamma_\mu + A_2^{(0)}\gamma_\mu\gamma_5\right)u(p_2) \qquad (28)$$
$$\times\left(\delta N_Z^\mu\, N_H + N_Z^\mu\,\delta N_H\right)\Big\}\frac{1}{D_Z(p_{34})D_H(p_{56})}\,,$$

with the denominators of the Z and Higgs-boson propagators defined by (10) and the amplitudes of the decay subprocesses given by

$$\begin{aligned} N_Z^\mu &= \bar{u}(k_4)\left(a_1^{(0)}\gamma^\mu + a_2^{(0)}\gamma^\mu\gamma_5\right)v(k_3)\,,\\ N_H &= g_{Hbb}^{(0)}\,\bar{u}(k_6)\,v(k_5) \end{aligned} \qquad (29)$$

in the lowest order and

$$\begin{aligned} \delta N_Z^\mu &= \bar{u}(k_4)\left(\delta a_1\gamma^\mu + \delta a_2\gamma^\mu\gamma_5\right)v(k_3)\,,\\ \delta N_H &= \delta g_{Hbb}\,\bar{u}(k_6)\,v(k_5) \end{aligned} \qquad (30)$$

in the one-loop and higher orders. Let us note that the invariant amplitudes δa_1, δa_2 and δg_{Hbb} contain the QED correction factors, which include the hard photon emission. We have neglected the so-called longitudinal part of the Z-boson propagator proportional to $p_{34}^\mu p_{34}^\nu$ in (27) and (28). Keeping this part would lead to some ambiguity, as the propagator couples to the final-state currents N_Z^μ and δN_Z^μ which are parameterized in terms of the projected momenta k_3 and k_4. The neglected term is of the order of m_μ, which is consistent with neglecting the $\mathcal{O}(m_\mu)$ terms in calculation of the one-loop EW decay amplitudes δa_1 and δa_2 of (30).

The invariant amplitudes of (28)[1]

$$\begin{aligned} &\delta A_i = \delta A_i(s,\cos\theta)\,, \qquad A_{ji} = A_{ji}(s,\cos\theta)\,,\\ &i=1,2\,,\quad j=3,4\,, \end{aligned} \qquad (31)$$

represent the IR finite parts of the EW one-loop correction to the on-shell Z–Higgs production process (1). They are complex functions of $s=(p_1+p_2)^2$ and $\cos\theta$, where θ is the Higgs-boson production angle with respect to the initial positron beam in the centre-of-mass system (CMS), computed with the program `eezh4f`. The latter makes use of the program worked out in [18] and the package `FF 2.0`. The package `FF` written by G.J. van Oldenborgh allows the evaluation of one-loop integrals [25]. Note that we have changed the notation a little in (28) with respect to that of (2.5) of [18]. The IR finite contributions to the EW one-loop form factors of the Zll-vertex δa_1, δa_1 and the correction δg_{Hbb} of the $Hb\bar{b}$-vertex of (30) are also calculated numerically following [21] and [22].

As the computation of the one-loop electroweak amplitudes of (31) slows down the MC integration substantially, a simple interpolation routine has been written that samples the amplitudes at a few hundred values of $\cos\theta$ and the amplitudes for all intermediate values of $\cos\theta$ are then obtained by linear interpolation. This gives a tremendous gain in the speed of computation, while there is practically no difference between the results obtained with the interpolation routine and without it.

[1] Only amplitudes that do not vanish in the limit $m_e \to 0$ are included.

We end this section with a description of the projection procedure we have applied in the program. The projected momenta k_Z and k_i, of (28), (29) and (30) are obtained from the four-momenta p_i, $i=3,\ldots,6$, of the final-state fermions of reaction (4) with the following projection procedure.

First the on-shell momenta and energies of the Higgs and Z boson in the CMS are fixed by

$$\begin{aligned} |\boldsymbol{k}_H| &= \frac{\lambda^{\frac{1}{2}}\left(s,m_Z^2,m_H^2\right)}{2s^{\frac{1}{2}}}\,, \quad \boldsymbol{k}_H = |\boldsymbol{k}_H|\,\frac{\boldsymbol{p}_5+\boldsymbol{p}_6}{|\boldsymbol{p}_5+\boldsymbol{p}_6|}\,,\\ E_H &= \left(\boldsymbol{k}_H^2+m_H^2\right)^{\frac{1}{2}}\,, \qquad \boldsymbol{k}_Z = -\boldsymbol{k}_H\,,\\ E_Z &= \sqrt{s}-E_H\,. \end{aligned} \qquad (32)$$

Next the four-momenta p_5 and p_3 of reaction (4) are boosted to the rest frame of the $b\bar{b}$- and $\mu^+\mu^-$-pairs, respectively, where they are denoted by p_5' and p_3'. The projected four-momenta k_i', $i=5,6$, in the rest frame of the $b\bar{b}$-pair are then obtained by the kinematical relations

$$\begin{aligned} |\boldsymbol{k'}_5| &= \frac{\lambda^{\frac{1}{2}}\left(m_H^2,m_5^2,m_6^2\right)}{2m_H}\,, \qquad \boldsymbol{k'}_5 = |\boldsymbol{k'}_5|\,\frac{\boldsymbol{p'}_5}{|\boldsymbol{p'}_5|}\,,\\ \boldsymbol{k'}_6 &= -\boldsymbol{k'}_5\,,\\ E'_i &= \left(\boldsymbol{k'}_i^2+m_i^2\right)^{\frac{1}{2}}\,, \quad i=5,6\,. \end{aligned} \qquad (33)$$

Similarly, one obtains k_3' and k_4' in the rest frame of the $\mu^+\mu^-$-pair using

$$\begin{aligned} |\boldsymbol{k'}_3| &= \frac{\lambda^{\frac{1}{2}}\left(m_Z^2,m_3^2,m_4^2\right)}{2m_Z}\,, \qquad \boldsymbol{k'}_3 = |\boldsymbol{k'}_3|\,\frac{\boldsymbol{p'}_3}{|\boldsymbol{p'}_3|}\,,\\ \boldsymbol{k'}_4 &= -\boldsymbol{k'}_3\,,\\ E'_i &= \left(\boldsymbol{k'}_i^2+m_i^2\right)^{\frac{1}{2}}\,, \quad i=3,4\,. \end{aligned} \qquad (34)$$

The four-momenta k_i', $i=3,\ldots,6$, are then boosted back to the CMS, giving the projected four-momenta k_i, $i=3,\ldots,6$ of $\mu^+,\mu^-,\bar{b}$ and b that satisfy the necessary on-shell relations

$$\begin{aligned} k_3^2 = k_4^2 = m_\mu^2\,, \qquad k_5^2 = k_6^2 = m_b^2\,,\\ (k_3+k_4)^2 = m_Z^2\,, \qquad (k_5+k_6)^2 = m_H^2\,. \end{aligned}$$

The actual value of $\cos\theta$ in (31) is given by $\cos\theta = k_H^3/|\boldsymbol{k}_H|$. The described projection procedure is not unique. As the Higgs-boson width is small, the ambiguity between the different possible projections is mainly related to the off-shell nature of the Z boson and is of the order of $\alpha\Gamma_Z/(\pi m_Z)$.

3 Numerical results

In this section, we will present a sample of numerical results for reaction (4) which have been obtained with the current version of the program `eezh4f`. Computations have been performed in the FWS with the Z boson mass, Fermi coupling and fine-structure constant in the Thomson limit as the initial SM EW physical parameters [26]:

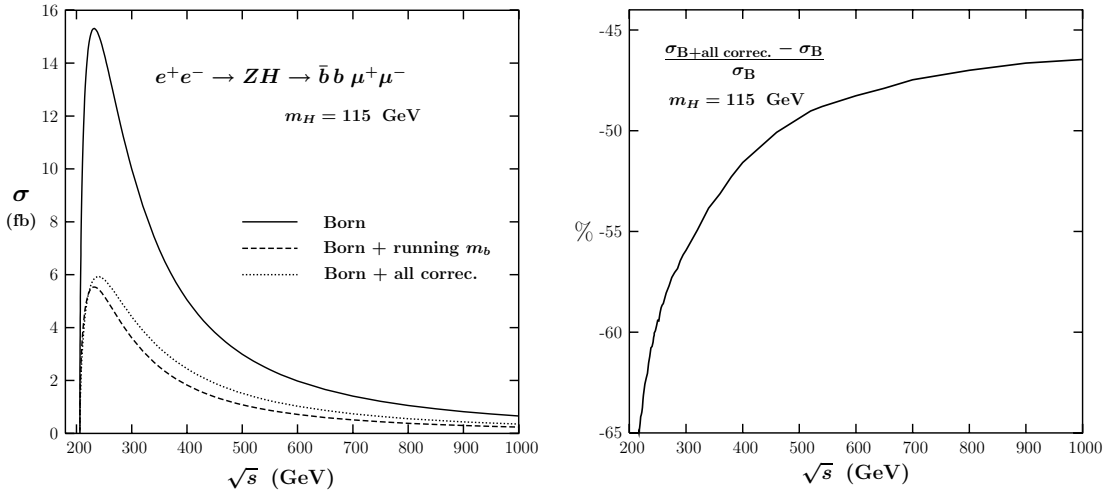

Fig. 3. The signal total cross section of reaction (4) in the NWA as a function of the CMS energy. The plots on the left show the Born cross section of (39) (solid line), the cross section of (40) (dashed line) and the cross section including all corrections as given by (42) (dotted line). The plot on the right shows the full relative correction with respect to the Born cross section

$$m_Z = 91.1876\,\text{GeV}\,, \qquad G_\mu = 1.16639 \times 10^{-5}\,\text{GeV}^{-2}\,,$$
$$\alpha_0 = 1/137.03599976\,. \tag{35}$$

The external particle masses of reaction (4) are the following:

$$m_e = 0.510998902\,\text{MeV}\,, \qquad m_\mu = 105.658357\,\text{MeV}\,,$$
$$m_b = 4.4\,\text{GeV}\,. \tag{36}$$

For definiteness, we give also values of the other fermion masses used in the computation:

$$\begin{aligned} m_\tau &= 1.77699\,\text{GeV}\,, & m_c &= 1.5\,\text{GeV}\,, \\ m_t &= 177.7\,\text{GeV}\,, & m_u &= 62\,\text{MeV}\,, \\ m_d &= 83\,\text{MeV}\,, & m_s &= 215\,\text{MeV}\,. \end{aligned} \tag{37}$$

The light-quark masses of (37), together with $\alpha_s = 0.123$, reproduce the hadronic contribution to the running of the fine-structure constant.

Assuming a specific value of the Higgs-boson mass, the W-boson mass and the total Z-boson width are calculated in a subroutine based on [21], while the total Higgs-boson width is calculated with HDECAY [22]. We obtain the following values for them for $m_H = 115\,\text{GeV}$ and the parameters specified in (35)–(37)

$$m_W = 80.40844\,\text{GeV}\,, \qquad \Gamma_Z = 2.50393\,\text{GeV}\,,$$
$$\Gamma_H = 2.8542\,\text{MeV}\,. \tag{38}$$

The total signal cross section of (4) in the narrow width approximation (NWA) is plotted on the left-hand side of Fig. 3 as a function of the CMS energy. The solid curve shows the Born cross section

$$\sigma^{\rm NWA}_{\rm Born} = \sigma^{(0)}_{e^+e^-\to ZH}\,\frac{\Gamma^{(0)}_{Z\to\mu^+\mu^-}}{\Gamma_Z}\,\frac{\Gamma^{(0)}_{H\to b\bar{b}}}{\Gamma_H}\,. \tag{39}$$

The dashed curve shows the cross section including the correction due to running of the b-quark mass

$$\sigma^{\rm NWA}_{\rm Born+running\,m_b} = \sigma^{(0)}_{e^+e^-\to ZH}\,\frac{\Gamma^{(0)}_{Z\to\mu^+\mu^-}}{\Gamma_Z}\,\frac{\Gamma^{\rm r.m.}_{H\to b\bar{b}}}{\Gamma_H}\,. \tag{40}$$

Finally, the dotted curve shows the cross section including the complete EW corrections to the Z–Higgs production and to the Z-boson decay width, as well as the QCD and EW corrections to the Higgs-boson decay width obtained with HDECAY and the ISR. The latter has been taken into account in the structure function approach by folding the cross section

$$\mathrm{d}\,\sigma^{\rm NWA} = \mathrm{d}\,\sigma_{e^+e^-\to\ ZH}\,\frac{\Gamma_{Z\to\mu^+\mu^-}}{\Gamma_Z}\,\frac{\Gamma_{H\to b\bar{b}}}{\Gamma_H} \tag{41}$$

with the structure function $\Gamma^{LL}_{ee}\left(x,Q^2\right)$ and integrating it over the full angular range according to

$$\begin{aligned} \sigma^{\rm NWA}_{\rm Born\,+\,all\,correc.} = &\int_0^1 \mathrm{d}x_1 \int_0^1 \mathrm{d}x_2 \Gamma^{LL}_{ee}\left(x_1,Q^2\right)\,\Gamma^{LL}_{ee}\left(x_2,Q^2\right) \\ &\times \int_{-1}^1 \mathrm{d}\cos\theta\,\frac{\mathrm{d}\sigma^{\rm NWA}}{\mathrm{d}\cos\theta}\left(x_1p_1, x_2p_2\right)\,, \end{aligned} \tag{42}$$

where x_1p_1 (x_2p_2) is the four-momentum of the positron (electron) after emission of a collinear photon. The structure function $\Gamma^{LL}_{ee}\left(x,Q^2\right)$ is given by (67) of [27], with BETA chosen for non-leading terms. The splitting scale Q^2, which is not fixed in the LL approximation is chosen to be equal $s = (p_1+p_2)^2$. The corresponding complete relative correction is plotted on the right-hand side of Fig. 3. It is large and dominated by the correction to the Higgs–$b\bar{b}$ Yukawa coupling caused by the running of m_b.

How the background Feynman diagram contribution and off-shell effects change the Higgsstrahlung signal cross section is illustrated in Fig. 4, where on the left (right) side we plot the total Born cross section of reaction (4) as a

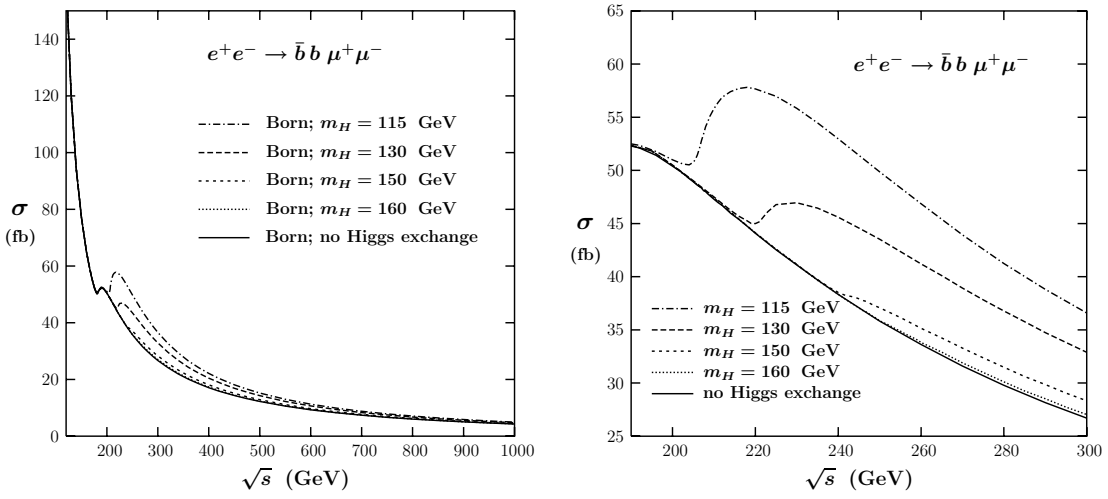

Fig. 4. The total Born cross section of reaction (4) as a function of the CMS energy in the energy range 120–1000 GeV (left) and 190–300 GeV (right) for different values of m_H

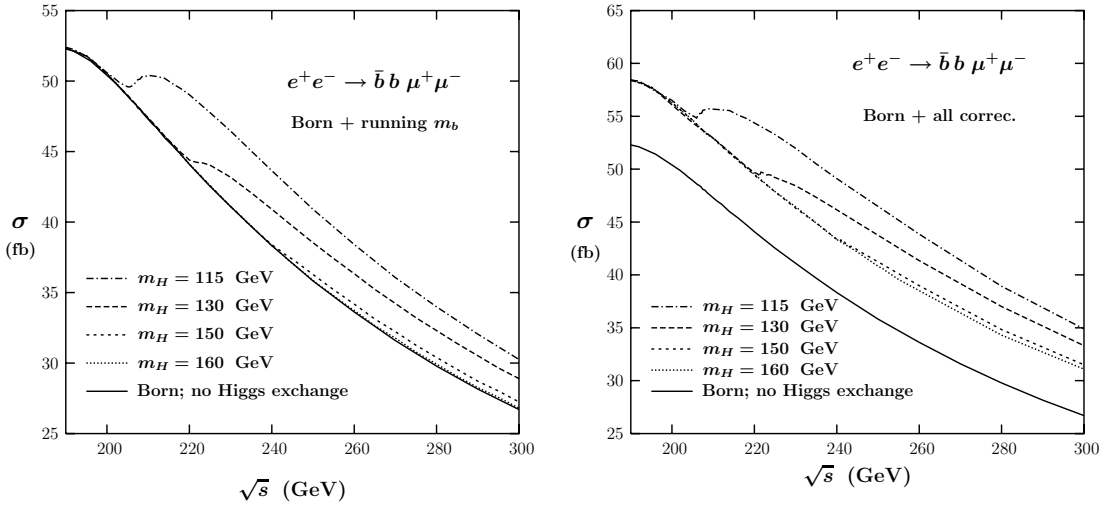

Fig. 5. The total cross section of reaction (4) as a function of the CMS energy for different values of m_H. The plots on the left include the correction $\delta g^{\mathrm{r.m.}}_{Hb\bar{b}}$ to the Higgs–$b\bar{b}$ Yukawa coupling caused by the running of the b-quark mass. The plots on the right include all the corrections of (6)

function of the CMS energy in the energy range 0.12–1 TeV (0.19–0.3 TeV) for a few different values of m_H. The Z–Higgs production signal that is clearly visible in Fig. 4 as a rise in the plots above the solid line, which represents the cross section of reaction (4) without the Higgs-boson exchange contribution, decreases while the Higgs mass is growing. For $m_H = 150$ GeV, it is already rather small, while it is hardly visible for $m_H = 160$ GeV. This effect is caused by the substantial growth of the total Higgs-boson width Γ_H with the growth of the Higgs-boson mass m_H. The latter results in a decrease of the branching ratio $\Gamma_{H\to b\bar{b}}/\Gamma_H$, as with growing m_H the Higgs decay into a W-boson pair starts to dominate. The first bump in the plots on the left-hand side of Fig. 4 reflects the double-Z production resonance.

The total cross sections of reaction (4) including radiative corrections are plotted in Fig. 5 as functions of the CMS energy in the range 190–300 GeV for a few selected values of the Higgs-boson mass. The plots on the left include the correction $\delta g^{\mathrm{r.m.}}_{Hb\bar{b}}$ to the Higgs–$b\bar{b}$ Yukawa coupling caused by the running of the b-quark mass, i.e., they depict the first integral on the right-hand side of (6). The correction is large and reduces the Higgsstrahlung signal substantially compared to the plots on the right-hand sight of Fig. 4. The plots on the right-hand side of Fig. 5 include all the corrections, as defined in (6). Compared to the corresponding plots on the left, they are shifted upwards with respect to the solid curve representing the Born cross section of reaction (4) without the Higgs-boson contribution. This is caused by taking into account the contribution from the initial-state bremsstrahlung with the hard-photon momentum integrated over the full phase space. As expected, inclusion of the ISR smears the Z–Higgs production signal.

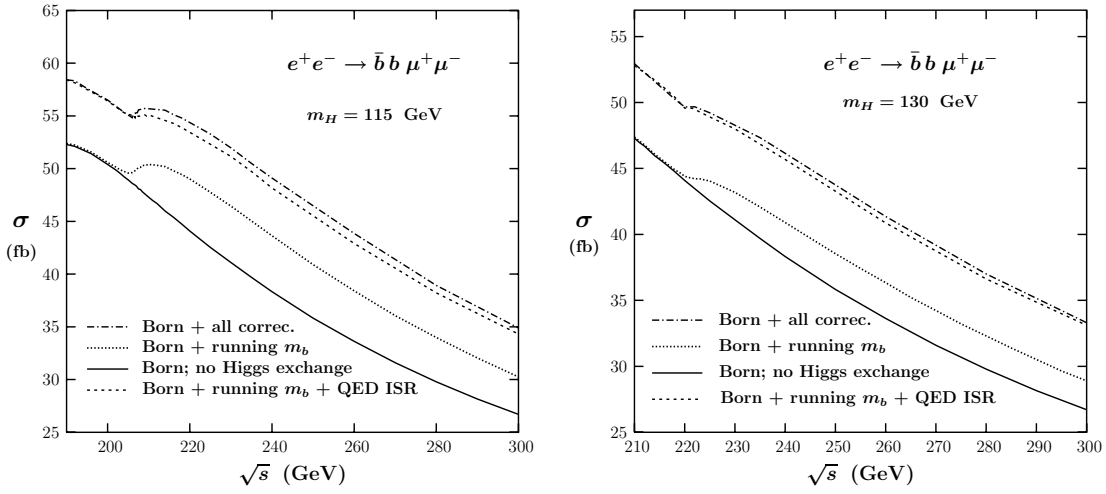

Fig. 6. The total cross section of reaction (4) for $m_H = 115\,\mathrm{GeV}$ (left) and $m_H = 130\,\mathrm{GeV}$ (right) including all the corrections (dashed–dotted line) as compared to the cross section including the QED ISR corrections and the correction due to the running of m_b, corresponding to the first three terms on the right-hand side of (6), (short dashed line). The plots of the Born cross section of reaction (4) without the Higgs-boson exchange (solid line) and the cross section of (4) including solely the correction due to the running of m_b (dotted line) are also shown

The size of EW corrections corresponding to the fourth term on the right-hand side of (6) can be read from Fig. 6, where the total cross section of reaction (4) for $m_H = 115\,\mathrm{GeV}$ (left) and $m_H = 130\,\mathrm{GeV}$ (right) including all the corrections (dashed–dotted line) and the cross section including the QED ISR corrections and the correction due to the running of m_b, corresponding to the first three terms on the right-hand side of (6), (short dashed line) are compared. The plots of the Born cross section of reaction (4) without the Higgs-boson exchange (solid line) and the cross section of (4) including solely the correction due to the running of m_b are also shown.

4 Summary and outlook

We have presented the SM predictions for a four-fermion reaction (4), which is one of the best detection channels of a low-mass Higgs boson produced through the Higgsstrahlung mechanism at a linear collider. We have included leading virtual and real QED ISR corrections to all the lowest-order Feynman diagrams of reaction (4). We have modified the lowest-order Higgs–$b\bar{b}$ Yukawa coupling in reactions (4) and (5) by including in it the correction to the Higgs-boson decay width caused by the running of the b-quark mass, which can be calculated with the program `HDECAY`. The complete $\mathcal{O}(\alpha)$ EW corrections to the Z–Higgs production and to the Z decay width, as well as the EW and remaining QCD corrections of `HDECAY`, have been taken into account in the double pole approximation. Moreover, we have illustrated how the Higgs-boson production signal is visible in the CMS dependence of the total cross section of reaction (4) for low Higgs masses and how it almost disappears as the Higgs mass approaches the W-pair decay threshold.

Some further work is required to include the non-factorizable corrections to reaction (4). Although, by comparison to the related process of ZZ production [23,24], one might expect that the non-factorizable corrections may largely cancel each other in the total cross section and may also be numerically suppressed in differential cross sections integrated over the decay angles for reaction (4), they should be included in the program to take into account properly the radiative corrections due to final-state real-photon radiation which, in the present work, have been included inclusively only in the EW one-loop corrections to the Z and Higgs-boson decay widths. To avoid possible negative-weight events which may occur in the MC simulation one should exponentiate the IR sensitive terms.

Acknowledgements. K.K. is grateful to the Alexander von Humboldt Foundation for supporting his stay at DESY Zeuthen, where this work has been accomplished and to the Theory Group of DESY Zeuthen for kind hospitality.

References

1. J. Erler, P. Langacker, in: PDG 2004, S. Eidelman et al., Phys. Lett. B **592**, 114 (2004)
2. R. Barate et al., Phys. Lett. B **565**, 61 (2003)
3. J.A. Aguilar-Saavedra et al. [ECFA/DESY LC Physics Working Group Collaboration], arXiv:hep-ph/0106315; T. Abe et al., [American Linear Collider Working Group Collaboration], arXiv:hep-ex/0106056; K. Abe et al. [ACFA Linear Collider Working Group Collaboration], arXiv:hep-ph/0109166
4. D.R.T. Jones, S.T. Petcov, Phys. Lett. B **84**, 440 (1979); R.L. Kelly, T. Shimada, Phys. Rev. D **23**, 1940 (1981); V. Barger, et al., Phys. Rev. D **49**, 79 (1994)
5. F. Jegerlehner, K. Kołodziej, T. Westwański, Nucl. Phys. Proc. Suppl. **135**, 92 (2004), arXiv:hep-ph/0407071
6. F.A. Berends, R. Pittau, R. Kleiss, Comput. Phys. Commun. **85**, 437 (1995)

7. A. Denner, S. Dittmaier, M. Roth, D. Wackeroth, Nucl. Phys. B **560**, 33 (1999); Comput. Phys. Commun. **153**, 462 (2003)
8. F. Jegerlehner, K. Kołodziej, Eur. Phys. J. C **23**, 463 (2002)
9. F. Krauss, R. Kuhn, G. Soff, JHEP **0202**, 044 (2002); A. Schalicke, F. Krauss, R. Kuhn, G. Soff, JHEP **0212**, 013 (2002)
10. E. Boos, M. Dubinin, Phys. Lett. B **308**, 147 (1993); G. Montagna, O. Nicrosini, F. Piccinini, Phys. Lett. B **348**, 496 (1995)
11. G. Passarino, Nucl. Phys. B **448**, 3 (1997)
12. A. Vicini, Acta Phys. Polon. B **29**, 2847 (1998)
13. F. Boudjema et al., Nucl. Phys. Proc. Suppl. **135**, 323 (2004), arXiv:hep-ph/0407079
14. A. Denner, S. Dittmaier, M. Roth, L.H. Wieders, arXiv:hep-ph/0502063; hep-ph/0505042
15. G. Belanger, et al., Nucl. Phys. Proc. Suppl. **116**, 353 (2003); G. Belanger, et al., Phys. Lett. B **559**, 252 (2003); A. Denner, S. Dittmaier, M. Roth, M.M. Weber, Phys. Lett. B **560**, 196 (2003); Nucl. Phys. B **660**, 289 (2003)
16. W. Beenakker, F.A. Berends, A.P. Chapovsky, Nucl. Phys. B **548**, 3 (1999); A. Denner, et al., Nucl. Phys. B **587**, 67 (2000); S. Jadach et al., Phys. Rev. D **61**, 113010 (2000)
17. K. Kołodziej, F. Jegerlehner, Comput. Phys. Commun. **159**, 106 (2004); arXiv:hep-ph/0308114
18. J. Fleischer, F. Jegerlehner, Nucl. Phys. B **216**, 469 (1983); BI-TP 87/04
19. B.A. Kniehl, Z. Phys. C **55**, 605 (1992); A. Denner, J. Küblbeck, R. Mertig, M. Böhm, Z. Phys. C **56**, 261 (1992)
20. See e.g. M. Consoli, S. Lo Presti, L. Maiani, Nucl. Phys. B **223**, 474 (1983); F. Jegerlehner, Z. Phys. C **32**, 425 (1986); A.A. Akhundov, D.Yu. Bardin, T. Riemann, Nucl. Phys. B **276**, 1 (1986); D.Yu. Bardin, S. Riemann, T. Riemann, Z. Phys. C **32**, 121 (1986)
21. F. Jegerlehner, in: Proceedings of the XI International School of Theoretical Physics, M. Zrałek and R. Mańka (eds.), World Scientific 1988, pp. 33–108
22. A. Djouadi, J. Kalinowski, M. Spira, Comput. Phys. Commun. **108**, 56 (1998)
23. W. Beenakker, A.P. Chapovsky, F.A. Berends, Nucl. Phys. B **560**, 33 (1999)
24. A. Denner, S. Dittmaier, M. Roth, Phys. Lett. B **429**, 145 (1998); Nucl. Phys. B **519**, 39 (1998)
25. G.J. van Oldenborgh, J.A.M. Vermaseren, Z. Physi C **46**, 425 (1990)
26. PDG 2004, S. Eidelman et al., Phys. Lett. B **592**, 114 (2004)
27. W. Beenakker et al., in: G. Altarelli, T. Sjöstrand, F. Zwirner (eds.), Physics at LEP2 (Report CERN 96-01, Geneva, 1996), Vol. 1, p. 79, hep-ph/9602351